APL Materials

Avalanches from charged domain wall motion in $BaTiO_3$ during ferroelectric switching

Cite as: APL Mater. **8**, 011105 (2020); https://doi.org/10.1063/1.5128892
Submitted: 23 September 2019 . Accepted: 17 December 2019 . Published Online: 10 January 2020

Blai Casals, Guillaume F. Nataf, David Pesquera, and Ekhard K. H. Salje

Avalanches from charged domain wall motion in $BaTiO_3$ during ferroelectric switching

Cite as: APL Mater. 8, 011105 (2020); doi: 10.1063/1.5128892
Submitted: 23 September 2019 • Accepted: 17 December 2019 •
Published Online: 10 January 2020

Blai Casals,[1] Guillaume F. Nataf,[2] David Pesquera,[1] and Ekhard K. H. Salje[1]

AFFILIATIONS

[1]Department of Earth Sciences, University of Cambridge, Downing Street, Cambridge CB2 3EQ, United Kingdom
[2]Department of Materials Science, University of Cambridge, 27 Charles Babbage Road, Cambridge CB3 0FS, United Kingdom

ABSTRACT

We report two methods for direct observations of avalanches in ferroelectric materials during the motion of domain walls. In the first method, we use optical imaging techniques to derive changes in domain structures under an electric field. All changes occur through small jumps (jerks) that obey avalanche statistics. In the second method, we analyze jerks by their displacement current. Both methods reveal a power law distribution with an energy exponent of 1.6, in agreement with previous acoustic emission measurements, and integrated mean field theory. This new combination of methods allows us to probe both polarization and strain variations during the motion of domain walls and can be used for a much wider class of ferroelectrics, including ceramic samples, than acoustic emission.

Domain boundary engineering,[1–3] where domain walls rather than domains are the active elements of a ferroic material, is extensively researched in condensed matter physics. The aim is to find domain walls exhibiting completely different physical properties compared with domains, such as polarity in nonpolar materials [$SrTiO_3$,[4,5] $CaTiO_3$,[6–8] $LaAlO_3$,[9] and $Pb_3(PO_4)_2$[10]] or enhanced conductivity in insulators [$BiFeO_3$,[11–15] $Nd_2Ir_2O_7$,[16] $ErMnO_3$,[17–20] $LiNbO_3$,[21–26] $Pb(Zr,Ti)O_3$,[27–29] $BaTiO_3$,[30,31] and for superconducting domain walls WO_3[32]]. Among these systems, $BaTiO_3$ domain walls stand alone because of the high magnitude of the conductivity recorded at room temperature.[30]

In order to take advantage of this metalliclike conductivity in a device, it is a requirement to know how to create, move, and erase domain walls at wish. For $BaTiO_3$, charged domain walls can be obtained by frustrative poling, e.g., by cooling a single crystal through its cubic to tetragonal phase transition while applying an electric field along the $[111]_c$ direction.[31] Domain walls can then be moved—and erased—by the application of an external electric field, e.g., along the $[-110]_c$ direction.

The motion of ferroelectric domain walls is a nonlinear dynamic process where ballistic propagation is often superimposed by sudden jumps called jerks.[33–35] Jerks give rise to noise in current measurements, as reported in $BaTiO_3$,[36–40] $Pb(Zr,Ti)O_3$[41] and $(Pb,La)(Zr,Ti)O_3$,[42] $(Pb,Mg)NbO_3$,[43] and $(Pb,Mg)NbO_3$-$PbTiO_3$.[39,44] Such jerks are initiated when walls are pinned and depinned in a stop-and-go mechanism. The sudden depinning gives rise to a sudden strain release which radiates acoustic signals. Similarly, jamming of domain walls emanates strain releases which can be measured as acoustic bursts. Jerks hence occur in both acoustic and electric measurements when domain walls are pinned by defects or because of depolarization fields resulting from local polarization charges.[45–47] Simulations show that they are also observed in the absence of extrinsic defects in the material and then result only from interactions between domain walls.[48,49] These processes do not depend on the scale of the energies involved where the same physical process occurs for small and big release mechanisms. This means that the dynamics of the domain switching is scale invariant. Jerks should exhibit all hallmarks of avalanche dynamics and, therefore, be described by power laws related to the probability to observe an avalanche with a certain energy.[50–53] Such relations for jerks in the displacement current during ferroelectric switching have been experimentally reported only in $Pb(Zr,Ti)O_3$[41] so far.

More specifically, the mobility of ferroelastic domain walls in ferroelectric materials depends on two order parameters, namely, polarization and strain, which are combined to define domain wall profiles. Therefore, avalanche dynamics can be probed through

changes in polarization, by measuring the displacement current,[36–44] but also through changes in strain, by recording acoustic emission.[54] Here, we study the prototypical ferroelectric $BaTiO_3$ in $(111)_c$ orientation for which charged domain walls have been reported using three complementary techniques: acoustic emission (previously reported in Ref. 54), current measurements, and optical microscopy, which allows us to "listen to, touch, and watch" the motion of the same ferroelectric domain walls. Optical microscopy gives a direct insight into the jerky motion of domain walls ("watch"), acoustic emission probe results of the strain fields ("listen"), and current measurement changes in polarization ("touch"). All three techniques combined allow us to probe the physics of domain wall avalanches as a whole.

We visualized the domain structure by measuring birefringence with an optical microscope in transmission mode. The experimental setup is sketched in Fig. 1(a): polarized white light is transmitted through the sample and an analyzer is used to select the polarization state before the CCD camera. In order to move domain walls, we applied an electric field along the $[-110]_c$ direction through two silver-paint electrodes on the sides of the sample. We used a picoammeter (Keithley 6487) to measure the displacement current of the sample while cycling the applied electric field.

In order to identify the direction of the ferroelectric polarization in the different domains, we set the polarizer at, respectively, 0° and 90° from the fixed position of the analyzer [Fig. 1(b), upper panel]. The contrast between domains at 0° and 90° is reversed, which indicates that the optical indicatrix is orthogonal between adjacent domains. Given the $[111]_c$ orientation of the sample and the fact that, at the surface, domain walls are parallel to the direction $[11\text{-}2]_c$, the change in contrast indicates that the polarization vectors in the domains are along the $[100]_c$ and $[010]_c$ axes. The comparison of images obtained on the upper and bottom surfaces of the sample, by changing the focus, reveals the same contrast with the same pattern [Fig. 1(b), bottom panel]. Domain walls are thus straight and normal to the $[-110]_c$ axis across the thickness of the sample.

We cycled the voltage between ±300 V at 0.1 V/s and 1 V/s (depending on the experiment) while measuring the displacement current and birefringence (12 frames/s). Figure 1(c) shows birefringence images taken at 0 V and 300 V for the increasing field and at 0 V and −300 V for decreasing field. On increasing the field, dark domains expand and bright domains shrink. This can only be understood if the bright and dark domains have polarization directions with opposite components along the direction of the applied field, i.e., [−110], from which we conclude that the domain walls are charged. The polarization direction in the domains can be determined using past studies of domain structures in $[111]_c$-oriented $BaTiO_3$.[30,31] The obtained domain structure remains stable on decreasing the voltage to 0 V, but on decreasing further, the domains move backward toward the initial state. Therefore, we observe two remanent states of the domain pattern, as expected for a ferroelectric material.[55]

We now focus on the dynamics of the observed domain wall motion. Birefringence images are divided into subregions [see Fig. 2(a)] for the analysis in order to prevent possible overlap between simultaneous avalanches and to increase the statistical significance by increasing the number of datasets. For each subregion, we compute the mean value of all pixel intensities as a function of time (μ). In order to increase the contrast, this calculation is performed with respect to the birefringence image at 0 V. Rather than being a smooth function of time, birefringence shows jerks, as shown in Fig. 2(b). We establish a dataset of all jerk amplitudes by computing the first derivate of the mean intensity value ($A_{Jerks} = d\mu/dt$) and of corresponding jerk energies by computing the square of the amplitudes ($E_{Jerks} = A^2_{jerks}$).[34] In Fig. 2(b) (bottom), we plot the energy: it shows few jerks with large energies and many small jerks with small energies.

In order to check if the energy jerks are power law distributed and follow the probability distribution function per energy interval $PDF(E) \sim E^{-\varepsilon}$, where ε is the energy exponent of avalanches, we use the maximum likelihood (ML)[56] method expressed in the following equation:

$$\hat{\varepsilon} = 1 + N_{E \geq E_0}\left[\sum_{i=1}^{N_{E \geq E_0}} \ln\left(\frac{E_i}{E_0}\right)\right], \quad (1)$$

where $\hat{\varepsilon}$ is the estimated energy exponent [maximum likelihood exponent (MLE)], E_0 is a varying energy cutoff, and $N_{E>E0}$ is the number of jerks with an energy equal or higher than E_0.

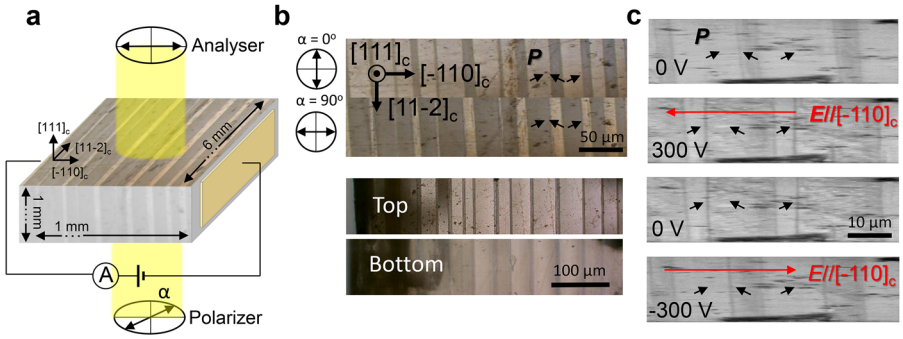

FIG. 1. (a) Sketch of the experimental setup: polarized white light is transmitted through the 1 × 6 × 1 mm^3 $BaTiO_3$ single crystal (field applied across 1 mm) and an analyzer is used to select the polarization state before the CCD camera. An electric field is applied along the $[-110]_c$, and displacement current is measured with a picoammeter. (b) The upper panel shows birefringence images for orthogonal angles of the polarizer (0° and 90°). The lower panel shows images for the same angle of the polarizer but with focus on top and bottom surfaces of the sample, respectively. (c) Evolution of the domain structure during ferroelectric switching at applied voltages of 0 V and 300 V on applying the field, 0 and −300 V on removing the field. In (b) and (c), arrows schematize the direction of the polarization in the domains.

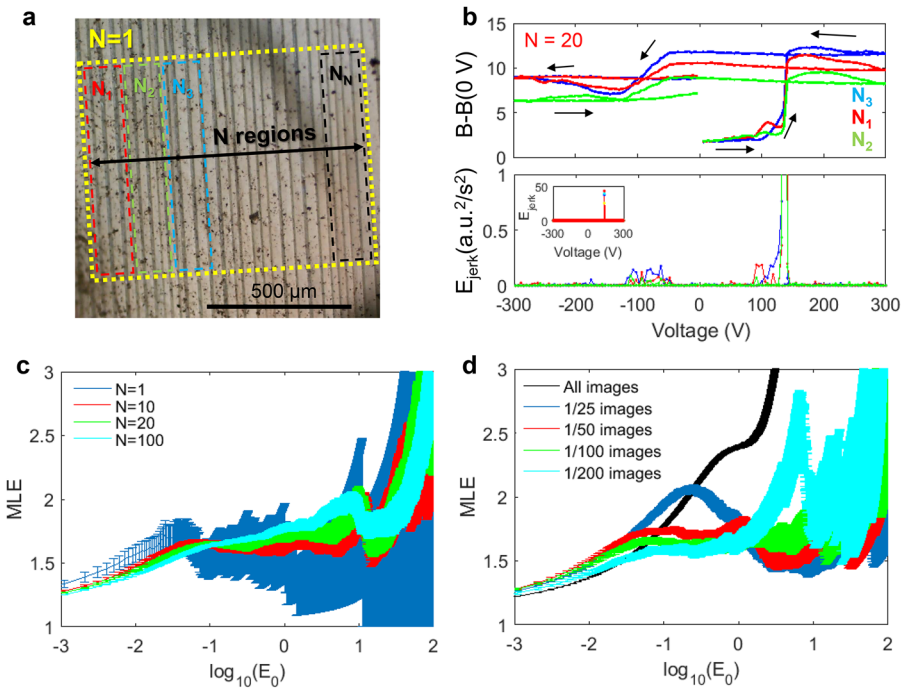

FIG. 2. (a) The birefringence image with divided areas in N subregions. N = 1 is the total area without any divisions. (b) Evolution of the birefringence under electric field with respect to the birefringence at 0 V and the corresponding energy jerks extracted from three subregions (N_1, N_2, and N_3) from 20 divisions of the total area. The jerk energy graph is enlarged to show the small energy jerks. The inset shows the jerk energies without enlargement where only the high energy jerks can be observed. (c) MLE obtained for a different number of regions. (d) images curtailed (for N = 20).

In our measurements, the experimental noise is comparable to the energy of the jerks. Therefore, to characterize the avalanche behavior of the domain wall motion, we developed two strategies. In the first one, we assess the statistical significance by computing the MLE of the jerks for an increasing number of subregions (N) corresponding to equal-spaced divisions of the same area [Fig. 2(a)]. When jerks are extracted from a single region covering all the sample (N = 1), as shown in Fig. 2(c), the MLE shows a plateau around ε = 1.6 with large error bar amplitudes (±0.5). With an increasing number of subregions, and as such datasets, the noise level is decreased by 80%. For 10 and 20 subregions, the plateau remains at 1.6. However, when the number of subregions is increased up to 100, the MLE exhibits a slope. This indicates that there are an optimal number of subregions for the determination of avalanche exponents. Indeed, for too few subregions, the overlap between avalanches and low statistic increases the noise in the MLE, while for too many subregions, a majority of avalanches occur across several subregions, which introduces an energy cutoff in the computed jerks and distorts the MLE plateau.[57]

Another strategy to reduce the amount of noise in the energy jerk spectra is to curtail the number of images per time as a low pass frequency filtering. Figure 2(d) shows the ML computed for a different number of images. If we analyze all images, i.e., the raw data (12 frames/s), the MLE curve shows a deflection around 2.4 and over less than 0.5 decades in energy. If we take 1 image every 25 frames, a peak appears on the MLE that we attribute to experimental noise. However, if we further increase the curtailing, this peak disappears. A plateau around 1.6 appears for 1 image every 50 frames and is preserved up to 1 image every 200 frames. However, for large rates such as 1/200, the energy range of the ML plateau is reduced from 3 decades (1/50) to 1 decade. Indeed, when we curtail the number of images per analysis, the amplitude of the computed jerks becomes larger than the experimental noise and the exponent exhibits a plateau, but when we skip too many images, many jerks are lost, reducing the statistical significance and the stability of the plateau. We conclude that there is an optimal curtailing, which is 1/100 in our case: at this value, the energy exponent converges at 1.6 and the energy plateau expands on several decades.

We now focus on the displacement current [Fig. 3(a)] measured simultaneously with the birefringence images discussed above. It shows the standard behavior of a ferroelectric material: a peak when increasing the voltage, caused by polarization switching, and another peak with the opposite sign when the voltage is reversed. The corresponding jerk energy is computed as the square of the first derivate of the current [Fig. 3(a), bottom]. Here, we have removed jerks originating from the smooth regions of the displacement current, which are artifacts. The MLE analysis exhibits a plateau around 1.6, in agreement with the plateau obtained from birefringence images [Fig. 3(b)]. However, the plateau expands over only one decade. Indeed, the magnitude of the displacement current depends on the amount of polarization switched per unit of time, and as such, low energy jerks are not measurable. Moreover, the displacement current is measured through the entire sample and the overlap between avalanches is more likely to occur. These circumstances reduce the energy range in which the measured jerks behave as a power law.

Figure 3(b) show the ML analysis for two voltage cycles where the voltage is increased at different rates. A plateau around 1.6 is observed for the rate of 1 V/s, in agreement with the simultaneous one obtained from birefringence images. There is no plateau at the rate of 0.1 V/s, suggesting that jerks are below the experimental noise level. The energy exponent obtained from birefringence is

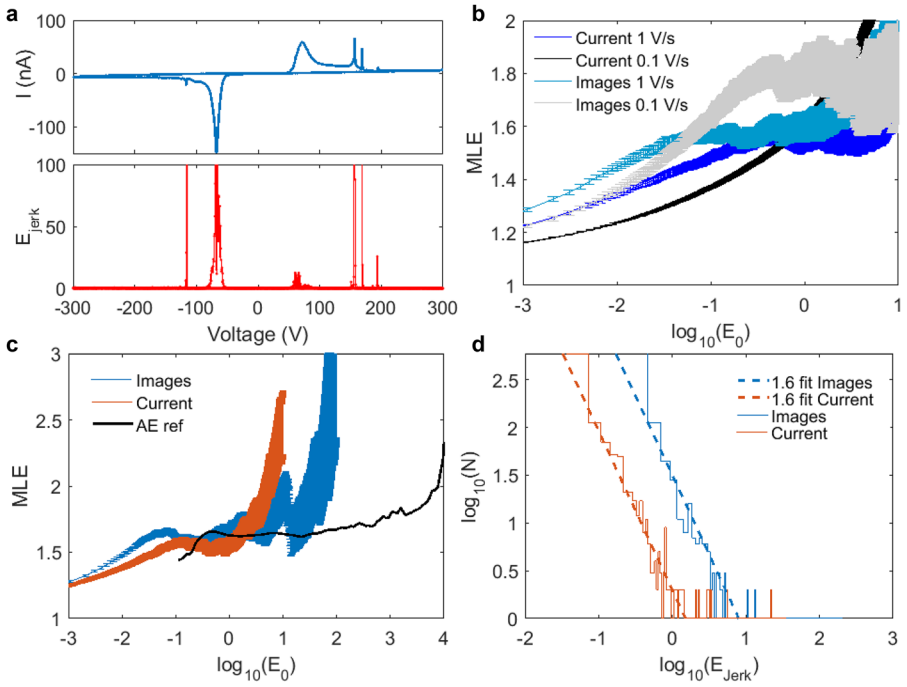

FIG. 3. (a) Evolution of the displacement current (I) under electric field and the corresponding energy jerks (E_{jerks}). (b) MLE for different rates of applied voltage obtained from the displacement current and birefringence images. (c) Comparison of MLE computed from birefringence images and displacement current with MLE obtained by acoustic emission (Ref. 54). (d) Log-log binning plot for the birefringence images and for the current. Straight lines indicate a slope of 1.6.

around 1.8, slightly higher than 1.6, caused by the combination of an increasing amount of lower energy jerks at a lower rate and the lack of statistics. For jerks in displacement current, these results indicate that the optimal rate has to be chosen such that overlap of avalanches is small (low rates) and events large enough to be detected (high rates). Despite this, the energy exponent obtained is similar to the one extracted from birefringence images.

In Fig. 3(c), we compared the MLE obtained from birefringence images, displacement current, and acoustic emission measurements on the same sample.[54] Additionally, we show in Fig. 3(d) the log-log binning for birefringence images and displacement current, which gives an energy exponent of 1.6. The expected mean field exponent for avalanches is 1.33.[50] The field-integrated mean field model predicts $\varepsilon = 1.67$,[50] which is very close to our experimental values. This indicates that domain wall switching follows a field-integrated pathway and that after each pinning or depinning event, an exponential relaxation follows as part of the avalanche. This exponential relaxation is observed in displacement current (polarization change), acoustic emission (strain change), and birefringence images (polarization and strain).

In summary, we used optical images and displacement current measurements to probe changes in polarization and strain induced by the motion of domain walls in $BaTiO_3$ $(111)_c$ during ferroelectric switching. We observed that domain wall motion is not smooth but occurs through jerks that exhibit all hallmarks of avalanche dynamics. The energy distribution of these jerks follows a power law with an exponent of 1.6, in agreement with previous acoustic emission measurements,[54] and with integrated mean field theory. The understanding of avalanches present at all length scales is critical for applications within the framework of domain boundary engineering, where a precise control of the position of domain walls is required.

This research was supported by a grant from EPSR (No. EP/P024904/1) to E.K.H.S., D.P., and B.C. G.F.N. thanks the Royal Commission for the Exhibition of 1851 for the award of a Research Fellowship.

REFERENCES

[1] E. K. H. Salje, ChemPhysChem **11**, 940 (2010).
[2] G. Catalan, J. Seidel, R. Ramesh, and J. F. Scott, Rev. Mod. Phys. **84**, 119 (2012).
[3] D. Meier, J. Phys.: Condens. Matter **27**, 463003 (2015).
[4] J. F. Scott, E. K. H. Salje, and M. A. Carpenter, Phys. Rev. Lett. **109**, 187601 (2012).
[5] E. K. H. Salje, O. Aktas, M. A. Carpenter, V. V. Laguta, and J. F. Scott, Phys. Rev. Lett. **111**, 247603 (2013).
[6] S. Van Aert, S. Turner, R. Delville, D. Schryvers, G. Van Tendeloo, and E. K. H. Salje, Adv. Mater. **24**, 523 (2012).
[7] H. Yokota, H. Usami, R. Haumont, P. Hicher, J. Kaneshiro, E. K. H. Salje, and Y. Uesu, Phys. Rev. B **89**, 144109 (2014).
[8] G. F. Nataf, M. Guennou, J. Kreisel, P. Hicher, R. Haumont, O. Aktas, E. K. H. Salje, L. Tortech, C. Mathieu, D. Martinotti, and N. Barrett, Phys. Rev. Mater. **1**, 074410 (2017).
[9] H. Yokota, S. Matsumoto, E. K. H. Salje, and Y. Uesu, Phys. Rev. B **98**, 104105 (2018).
[10] H. Yokota, S. Matsumoto, E. K. H. Salje, and Y. Uesu, Phys. Rev. B **100**, 024101 (2019).
[11] J. Seidel, L. W. Martin, Q. He, Q. Zhan, Y.-H. Chu, A. Rother, M. E. Hawkridge, P. Maksymovych, P. Yu, M. Gajek, N. Balke, S. V. Kalinin, S. Gemming, F. Wang, G. Catalan, J. F. Scott, N. A. Spaldin, J. Orenstein, and R. Ramesh, Nat. Mater. **8**, 229 (2009).
[12] S. Farokhipoor and B. Noheda, Phys. Rev. Lett. **107**, 127601 (2011).
[13] J. Seidel, P. Maksymovych, Y. Batra, A. Katan, S.-Y. Yang, Q. He, A. P. Baddorf, S. V. Kalinin, C.-H. Yang, J.-C. Yang, Y.-H. Chu, E. K. H. Salje, H. Wormeester, M. Salmeron, and R. Ramesh, Phys. Rev. Lett. **105**, 197603 (2010).
[14] Z. L. Bai, X. X. Cheng, D. F. Chen, D. W. Zhang, L. Chen, J. F. Scott, C. S. Hwang, and A. Q. Jiang, Adv. Funct. Mater. **28**, 1801725 (2018).

[15]T. Rojac, A. Bencan, G. Drazic, N. Sakamoto, H. Ursic, B. Jancar, G. Tavcar, M. Makarovic, J. Walker, B. Malic, and D. Damjanovic, Nat. Mater. **16**, 322 (2016).
[16]E. Y. Ma, Y.-T. Cui, K. Ueda, S. Tang, K. Chen, N. Tamura, P. M. Wu, J. Fujioka, Y. Tokura, and Z.-X. Shen, Science **350**, 538 (2015).
[17]D. Meier, J. Seidel, A. Cano, K. Delaney, Y. Kumagai, M. Mostovoy, N. A. Spaldin, R. Ramesh, and M. Fiebig, Nat. Mater. **11**, 284 (2012).
[18]J. Schaab, I. P. Krug, F. Nickel, D. M. Gottlob, H. Doğanay, A. Cano, M. Hentschel, Z. Yan, E. Bourret, C. M. Schneider, R. Ramesh, and D. Meier, Appl. Phys. Lett. **104**, 232904 (2014).
[19]P. Schoenherr, K. Shapovalov, J. Schaab, Z. Yan, E. D. Bourret, M. Hentschel, M. Stengel, M. Fiebig, A. Cano, and D. Meier, Nano Lett. **19**, 1659 (2019).
[20]J. Schaab, A. Cano, M. Lilienblum, Z. Yan, E. Bourret, R. Ramesh, M. Fiebig, and D. Meier, Adv. Electron. Mater. **2**, 1500195 (2016).
[21]M. Schröder, A. Haußmann, A. Thiessen, E. Soergel, T. Woike, and L. M. Eng, Adv. Funct. Mater. **22**, 3936 (2012).
[22]M. Schröder, X. Chen, A. Haußmann, A. Thiessen, J. Poppe, D. A. Bonnell, and L. M. Eng, Mater. Res. Express **1**, 035012 (2014).
[23]C. Godau, T. Kämpfe, A. Thiessen, L. M. Eng, and A. Haußmann, ACS Nano **11**, 4816 (2017).
[24]A.-S. Pawlik, T. Kämpfe, A. Haußmann, T. Woike, U. Treske, M. Knupfer, B. Büchner, E. Soergel, R. Streubel, A. Koitzsch, and L. M. Eng, Nanoscale **9**, 10933 (2017).
[25]T. Kämpfe, P. Reichenbach, M. Schröder, A. Haußmann, L. M. Eng, T. Woike, and E. Soergel, Phys. Rev. B **89**, 035314 (2014).
[26]G. F. Nataf, M. Guennou, A. Haußmann, N. Barrett, and J. Kreisel, Phys. Status Solidi RRL **10**, 222 (2016).
[27]J. Guyonnet, I. Gaponenko, S. Gariglio, and P. Paruch, Adv. Mater. **23**, 5377 (2011).
[28]I. Gaponenko, P. Tückmantel, J. Karthik, L. W. Martin, and P. Paruch, Appl. Phys. Lett. **106**, 162902 (2015).
[29]A. Tselev, P. Yu, Y. Cao, L. R. Dedon, L. W. Martin, S. V. Kalinin, and P. Maksymovych, Nat. Commun. **7**, 11630 (2016).
[30]T. Sluka, A. K. Tagantsev, P. Bednyakov, and N. Setter, Nat. Commun. **4**, 1808 (2013).
[31]P. S. Bednyakov, T. Sluka, A. K. Tagantsev, D. Damjanovic, and N. Setter, Sci. Rep. **5**, 15819 (2015).
[32]A. Aird and E. K. H. Salje, J. Phys.: Condens. Matter **10**, L377 (1998).
[33]V. Y. Shur, E. V. Nikolaeva, E. L. Rumyantsev, E. I. Shishkin, A. L. Subbotin, and V. L. Kozhevnikov, Ferroelectrics **222**, 323 (1999).
[34]R. J. Harrison and E. K. H. Salje, Appl. Phys. Lett. **97**, 021907 (2010).
[35]S. Puchberger, V. Soprunyuk, W. Schranz, A. Tröster, K. Roleder, A. Majchrowski, M. A. Carpenter, and E. K. H. Salje, APL Mater. **5**, 046102 (2017).
[36]V. M. Rudyak, Sov. Phys. - Usp. **13**, 461 (1971).
[37]R. C. Miller, Phys. Rev. **111**, 736 (1958).
[38]A. G. Chynoweth, J. Appl. Phys. **30**, 280 (1959).
[39]Y. Xu, D. Xue, Y. Zhou, T. Su, X. Ding, J. Sun, and E. K. H. Salje, Appl. Phys. Lett. **115**, 022901 (2019).
[40]D. Pesquera, B. Casals, J. E. Thompson, G. F. Nataf, X. Moya, and M. A. Carpenter, APL Mater. **7**, 051109 (2019).
[41]C. D. Tan, C. Flannigan, J. Gardner, F. D. Morrison, E. K. H. Salje, and J. F. Scott, Phys. Rev. Mater. **3**, 034402 (2019).
[42]G. Pleyber, K. Biedrzycki, and R. Le Bihan, Ferroelectrics **141**, 125 (1993).
[43]E. V. Colla, L. K. Chao, and M. B. Weissman, Phys. Rev. Lett. **88**, 017601 (2002).
[44]X. Zhang, C. Mellinger, E. V. Colla, M. B. Weissman, and D. D. Viehland, Phys. Rev. B **95**, 144203 (2017).
[45]B. Tadić, Eur. Phys. J. B **28**, 81 (2002).
[46]S. Liu, I. Grinberg, and A. M. Rappe, Nature **534**, 360 (2016).
[47]V. Y. Shur, E. L. Rumyantsev, D. V. Pelegov, V. L. Kozhevnikov, E. V. Nikolaeva, E. L. Shishkin, A. P. Chernykh, and R. K. Ivanov, Ferroelectrics **267**, 347 (2002).
[48]X. Ding, T. Lookman, E. K. H. Salje, and A. Saxena, JOM **65**, 401 (2013).
[49]E. K. H. Salje, X. Ding, Z. Zhao, and T. Lookman, Appl. Phys. Lett. **100**, 222905 (2012).
[50]E. K. H. Salje and K. A. Dahmen, Annu. Rev. Condens. Matter Phys. **5**, 233 (2014).
[51]N. Friedman, A. T. Jennings, G. Tsekenis, J.-Y. Kim, M. Tao, J. T. Uhl, J. R. Greer, and K. A. Dahmen, Phys. Rev. Lett. **109**, 095507 (2012).
[52]K. A. Dahmen, Y. Ben-Zion, and J. T. Uhl, Phys. Rev. Lett. **102**, 175501 (2009).
[53]J. P. Sethna, K. A. Dahmen, and C. R. Myers, Nature **410**, 242 (2001).
[54]E. K. H. Salje, D. Xue, X. Ding, K. A. Dahmen, and J. F. Scott, Phys. Rev. Mater. **3**, 014415 (2019).
[55]O. Vlasin, B. Casals, N. Dix, D. Gutiérrez, F. Sánchez, and G. Herranz, Sci. Rep. **5**, 15800 (2015).
[56]A. Clauset, C. R. Shalizi, and M. E. J. Newman, SIAM Rev. **51**, 661 (2009).
[57]J. T. Uhl, S. Pathak, D. Schorlemmer, X. Liu, R. Swindeman, B. A. W. Brinkman, M. LeBlanc, G. Tsekenis, N. Friedman, R. Behringer, D. Denisov, P. Schall, X. Gu, W. J. Wright, T. Hufnagel, A. Jennings, J. R. Greer, P. K. Liaw, T. Becker, G. Dresen, and K. A. Dahmen, Sci. Rep. **5**, 16493 (2015).